DOI: 10.21791/IJEMS.2026.09

Research Paper

Effects of Surface Grinding Parameters on the Apparent Elastic Modulus of AA7075 Thin Plate

Michael Boadu[1], Anthony Agyei-Agyemang[2], Faisal Adam[2]

[1]University for Development Studies, School of Engineering, Department of Mechanical and Industrial Engineering, Tamale, Ghana. boadumian@gmail.com (corresponding author)
[2]Kwame Nkrumah University of Science and Technology, College of Engineering, Department of Mechanical Engineering, Kumasi, Ghana. aaagyemang.coe@knust.edu.gh
[2]Kwame Nkrumah University of Science and Technology, College of Engineering, Department of Mechanical Engineering, Kumasi, Ghana. fwahibadam.coe@knust.edu.gh

Received: 2 Jan 2026 **Accepted:** 1 June 2026 **Online Publication Date**: 1 June 2026

How to cite

M. K. Boadu, A. Agyei-Agyemang and F. Adam," Effects of Surface Grinding Parameters on the Apparent Elastic Modulus of AA7075 Thin Plate", *International Journal of Engineering and Management Sciences*, pp. 1–20., June 2026. doi: 10.21791/IJEMS.2026.09

Abstract. Aluminum 7075 (AA7075) thin plates are used extensively in the marine industry, especially for the manufacture of skin panels for hydrofoils. Although surface grinding is a finishing process for AA7075 thin plates, the extent of the influence of grinding parameters on the apparent elastic modulus is not well understood. This study statistically evaluates the influence of surface grinding parameters on the apparent elastic modulus of AA7075 thin plates. Samples of AA7075 thin plates were ground with respect to an experimental design, and their apparent elastic modulus was measured from the DI-CP/V2 Servo-hydraulic testing machine. It was found that the feed has the highest standardized effect (7.0) on the apparent elastic modulus (9.84–32.81 GPa), followed by table speed (5.8) and grinding depth (5.5). The two-way interactions were significant except for the table speed-grinding depth interaction. The regression model shows a close match to the experimental data as indicated by the low standard error (S = 2.14), large coefficient of determination (R^2 = 82.51%), and high adjusted coefficient of determination (R^2 adj = 73.52%), which means that the chosen factors and interactions can be used to explain the large percentage of the variability of the apparent elastic modulus. The optimal grinding parameters were found at high table speed (50 spm), high feed (5 mm), and high grinding depth (1 mm).

Keywords: Statistical Evaluation, Surface Grinding Parameters, Apparent Elastic Modulus, AA7075 Thin Plates.

Introduction

Aluminum (Al) and its alloys are widely utilized across numerous engineering sectors. Aluminum 7075 is the most widely produced and used alloy among them due to its excellent mechanical properties, including high tensile strength, high impact resistance, and wear resistance, especially in the automotive and aerospace industry [1].

DOI: 10.21791/IJEMS.2026.09

Grinding is a complex material removal process, where cutting, ploughing and rubbing are involved, and the proportions of the three actions are dependent on the interaction between the abrasive grains and the workpiece material [2]. As reported by Singh et al. [3], grinding accounts for about 43% of all machining operations in the manufacturing industry, indicating that it is a widely used machining technique.

Modulus of Elasticity, also known as Elastic Modulus or simply modulus, is the measurement of a material's elasticity. Elastic Modulus quantifies a material's resistance to non-permanent, or elastic deformation [4]. According to Hill [5], the elastic modulus measures the stiffness of materials and their ability to resist deformation when subjected to tensile stress. It quantifies how much a material will stretch or compress under an applied force. When the elastic modulus is not compliance corrected, it is referred to as the apparent elastic modulus.

Boadu et al. [6] assessed the trends in the elastic modulus of AA7075 thin plate subjected to surface grinding across 54 run orders. The elastic modulus varied between 10 and 33 GPa, with mid-run fluctuations and stabilization toward the final runs.

Hou et al. [7] reported that an increase in the depth of cut and the grinding wheel speed or a decrease in the workpiece speed leads to a thicker grind-hardening layer of steel GCr15. They suggested that to increase the hardness penetration depth, a larger depth of cut, grinding wheel speed, and smaller workpiece speed should be selected, under the internal grind-hardening experimental conditions.

Guo et al. [8] reported that micro-grains are refined into equiaxed nano-grains in Al6061T6 workpieces subjected to grinding. They observed that continuous dynamic recrystallization is induced at a decreasing depth with an increasing grinding speed due to the high strain-rate field and the reduced depth of the heat affected layer, which encourages the phenomenon of damage skin effect.

Beghini et al. [9] reported that increasing the feed rate results in higher surface hardness, while its influence on the elastic modulus becomes negligible at greater material depths.

Experimental design provides an organized approach to systematically investigate the influence of several factors on surface quality, and it can be used to develop general surface models that reliably predict surface quality [10]. A major advantage of the factorial design is that it can be used to study multiple independent variables simultaneously without running separate experiments for each. Moreover, factorial design can determine and analyze interaction effects of the studied variables [11].

There is limited studies on the effect of surface grinding parameters on the apparent elastic modulus, particularly from a statistical perspective. Elastic modulus is one of the parameters affecting stiffness and structural responses, the sensitivity of the parameter to surface grinding conditions is needed, particularly for thin plates, where the sensitivity is stronger. Furthermore, there are no statistically validated models that quantify the individual and interactive effects of the grinding parameters, which can be seen as a gap in process–property optimization. This study addresses this gap through a systematic statistical evaluation of surface grinding parameters influencing the apparent elastic modulus of AA7075 thin plates.

DOI: 10.21791/IJEMS.2026.09

1. Material and Methods

The material employed in this study was an AA7075 thin plate, and it was obtained from B5 Plus Group in Kumasi, Ghana, and its chemical composition is presented in Table 1. The measured density was 2.77 g/cm^3, while the mechanical properties of the as-received AA7075 thin plate are summarized in Table 2. The apparent elastic modulus for the as-received AA7075 sample is lower in comparison to standard values due to the thickness effect and specimen geometry. During tensile testing, thin plates are more likely to be subject to a slight out-of-plane deformation, local buckling, and bending. Such effects decrease the apparent stiffness response and are more significant for thin specimens than for bulk materials. Mechanical property testing of the as-received material was carried out using three specimens. The original gauge length, L_0 was 200 mm and the thickness was 4 mm. The width and length of each plate were 50 mm and 300 mm, respectively. The servo-hydraulic testing machine was employed to conduct uniaxial tensile tests. The results were averaged to obtain representative mechanical properties for the as-received sample. The standard deviation was computed for each property.

Element	Si	Fe	Zn	Mg	Ti	Cu	Cr	Mn	Pb	Al
% by weight	≤0.40	≤0.50	5.1-6.1	2.1–2.9	≤0.20	1.2-2.0	0.18-0.28	≤0.3	≤0.05	≥89.97

Table 1. Chemical composition of AA7075 [12]

Mechanical properties	Mean	Standard deviation
Tensile strength,σ_t, MPa	157.7	0.80
Yield strength σ_Y, MPa	146.1	0.56
Total elongation E_l, %	9.4	0.26
Uniform elongation El_u, %	4.2	0.20
Young modulus *E*, GPa	14.08	0.06

Table 2. Mechanical properties of the as-received AA7075 sample

1.1. Design of experiment

A 3^3 full factorial design was adopted for the experimental investigation. To enhance reliability, each experimental condition was replicated twice, resulting in a total of 54 experimental runs. The 3^3 factorial design matrix is presented in Table 3, while the complete experimental layout is detailed in Table 4. The factor levels for table speed (Vs), feed (f), and grinding depth (d) were selected based on the operational limits of the available grinding machine.

Independent Variables	Low (0)	Medium (1)	High (2)
Table Speed, Vs (spm)	2.0	15.0	50.0
Feed, f (mm)	1.0	2.0	5.0
Grinding Depth, d (mm)	0.2	0.5	1.0

Table 3. The 3^3 experimental design levels

These parameter ranges were sufficiently broad to capture measurable variations in tensile strength, yield strength, apparent elastic modulus, and elongation, yet conservative enough to prevent excessive tool wear, thermal damage, or surface defects. Furthermore, the chosen experimental settings ensured efficient execution of the tests within laboratory time constraints while maintaining repeatability and

DOI: 10.21791/IJEMS.2026.09

operational safety. The geometrical representation of a 3^3 factorial design is shown in Fig. 1. The numbers denote the experimental runs.

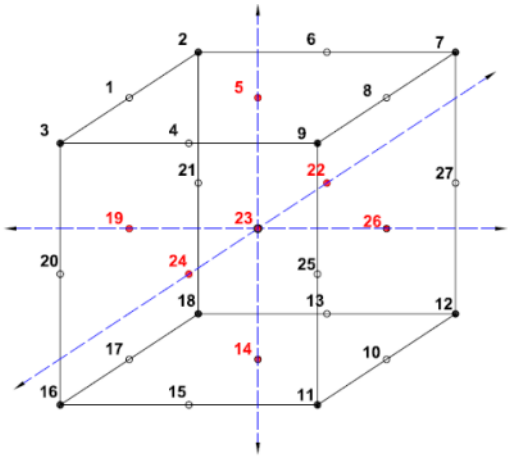

Figure 1. Geometric illustration of 3^3 factorial design [13]

Runs	Vs (spm)	f (mm)	d (mm)
1, 28	2	1	0.2
2. 29	15	1	0.2
3, 30	50	1	0.2
4, 31	2	2	0.2
5, 32	15	2	0.2
6, 33	50	2	0.2
7, 34	2	5	0.2
8, 35	15	5	0.2
9, 36	50	5	0.2
10, 37	2	1	0.5
11, 38	15	1	0.5
12, 39	50	1	0.5
13, 40	2	2	0.5
14, 41	15	2	0.5
15, 42	50	2	0.5
16, 43	2	5	0.5
17, 44	15	5	0.5
18, 45	50	5	0.5
19, 46	2	1	1
20, 47	15	1	1
21, 48	50	1	1
22, 49	2	2	1
23, 50	15	2	1
24, 51	50	2	1
25, 52	2	5	1
26, 53	15	5	1
27, 54	50	5	1

Table 4. Detailed 3^3 experimental design with levels and runs

DOI: 10.21791/IJEMS.2026.09

1.2. Sample Preparation for Tensile Test

The specimens were prepared in accordance with the relevant international standard [14]. A total of 54 specimens were used for the tensile tests, all of which were extracted from the parent plate using a 750 W Total angle grinder operating at a no-load speed of 12,000 rpm and a rated voltage of 220–240 V. Cutting was performed carefully at room temperature to avoid any alteration of the material's inherent properties. The original thickness was 4 mm. The specimens had an initial gauge length (L_0) of 200 mm, a plate width of 50 mm, and an overall length of 300 mm, resulting in a cross-sectional area (S_0) of 200 mm^2. An unmachined test specimen illustrating the plate's cross-sectional area is shown in Figure 2. An image showing samples of as-received thin plates after preparation is presented in Figure 3.

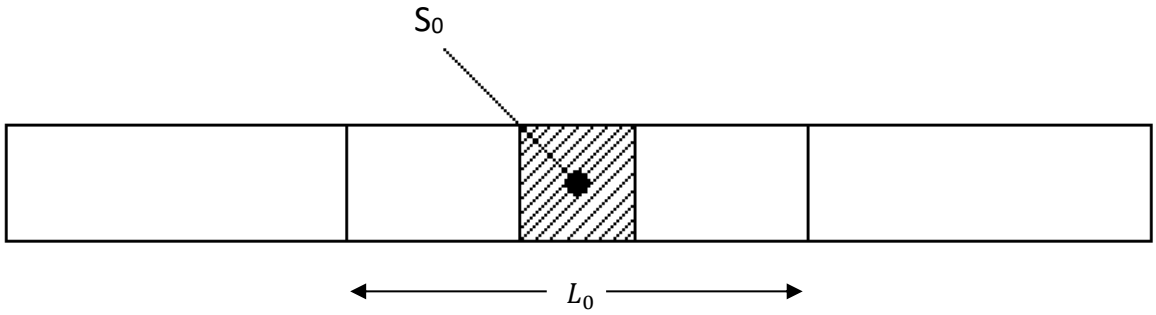

Figure 2. Cross-section of unmachined test piece

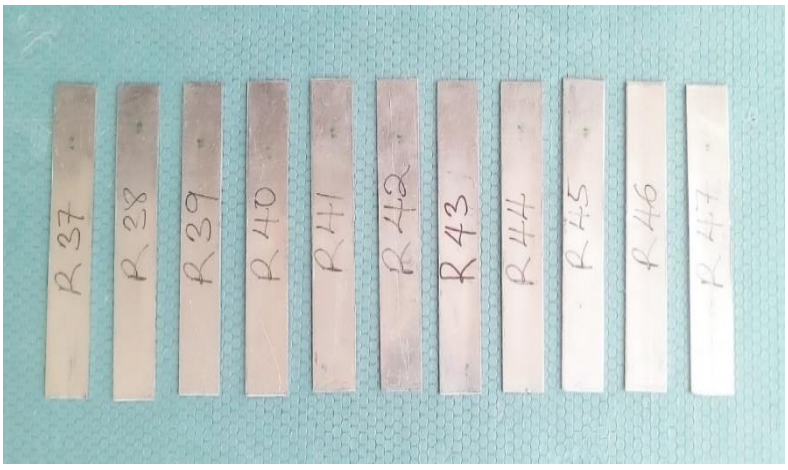

Figure 3. Samples of AA7075 thin plate after preparation

1.3. Experimental procedure for tensile test of aluminum 7075 thin plates

Surface grinding was carried out at room temperature using an Elliot 921 hydraulic surface grinding machine fitted with a diamond grinding wheel of 80 μm grit size, producing final plate thicknesses of 3.0 mm, 3.5 mm, and 3.8 mm. The grinding wheel speed was maintained at 2140.0 rpm, while the grinding parameters—table speed, feed rate, and grinding depth—were varied according to the experimental design presented in Table 3.

DOI: 10.21791/IJEMS.2026.09

Figure 4. Experimental set-up for the tensile test

Figure 5. (a) Unfractured sample before the test

(b) A fractured sample after the test

All grinding operations were performed under dry conditions with no coolant applied. Following surface grinding, cross-sectional areas (S_0) of 150 mm^2**,** 175 mm^2, and 190 mm^2 were obtained. Subsequently, tensile testing was conducted in accordance with the relevant international standard [14]. The tests were performed using a DI-CP/V2 servo-hydraulic universal testing machine equipped with a 2000 kN load cell, operating at ambient temperature and a constant travel distance of 900 mm. The cross-head displacement method was employed to measure strain. Each specimen was carefully aligned and secured in the grips before loading. A monotonically increasing tensile load was applied until fracture occurred, and the apparent elastic modulus values were automatically computed by the machine's software. This procedure was repeated for all remaining specimens.

DOI: 10.21791/IJEMS.2026.09

1.4. Analysis of Statistical Data

1.4.1. The 3^3 design model

The 3^3 design model consists of three factors, each at three levels. The model for such an experiment is given as follows:

$$Y_{ijk} = \mu + A_i + B_j + AB_{ij} + C_k + AC_{ik} + BC_{jk} + ABC_{ijk} + \varepsilon_{ijk} \quad (1)$$

Where Y_{ijk} denotes the observed response (e.g., apparent elastic modulus), μ represents the overall mean or intercept, corresponding to the average response across all observations and independent of treatment effects. A_i corresponds to the effect of the *i*th level of factor A (table speed), while B_j represents the effect of the *j*th level of factor B (feed). The term AB_{ij} denotes the interaction effect between the *i*th level of factor A and the *j*th level of factor B. Similarly, C_k represents the effect of the *k*th level of factor C (grinding depth), AC_{ik} denotes the interaction between the *i*th level of factor A and the *k*th level of factor C, and BC_{jk} represents the interaction between the *j*th level of factor B and the *k*th level of factor C. The three-factor interaction among table speed, feed, and grinding depth is expressed by ABC_{ijk}. Finally, ε_{ijk} denotes the random error term associated with (Y_{ijk}), which is assumed to be independently and identically distributed with a mean of zero and a variance $(0, \sigma^2)$.

1.4.2. Estimation of Parameters

Analysis of specific factor effects requires estimating parameters in ANOVA models, including blocks, treatment effects, interaction terms, error, and total variation [15]. The average response of each level of factor A is as follows:

$$\bar{A}_1 = {}^1/_9 \sum_{j=1}^{3}\sum_{k=1}^{3} Y_{1jk} \quad (2)$$

$$\bar{A}_2 = {}^1/_9 \sum_{j=1}^{3}\sum_{k=1}^{3} Y_{2jk} \quad (3)$$

$$\bar{A}_3 = {}^1/_9 \sum_{j=1}^{3}\sum_{k=1}^{3} Y_{3jk} \quad (4)$$

The main effect of each level of factor A is as follows:

$$A_1 = \bar{A}_1 - \bar{Y} \quad (5)$$

$$A_2 = \bar{A}_2 - \bar{Y} \quad (6)$$

$$A_3 = \bar{A}_3 - \bar{Y} \quad (7)$$

Where $\bar{Y}$ is the average of the responses for all treatments.

DOI: 10.21791/IJEMS.2026.09

The average response of each level of factor B is as follows:

$$\bar{B}_1 = {}^1/_9 \sum_{i=1}^{3} \sum_{k=1}^{3} Y_{1ik} \tag{8}$$

$$\bar{B}_2 = {}^1/_9 \sum_{i=1}^{3} \sum_{k=1}^{3} Y_{2ik} \tag{9}$$

$$\bar{B}_3 = {}^1/_9 \sum_{i=1}^{3} \sum_{k=1}^{3} Y_{3ik} \tag{10}$$

The main effect of each level of factor B is as follows:

$$B_1 = \bar{B}_1 - \bar{Y} \tag{11}$$

$$B_2 = \bar{B}_2 - \bar{Y} \tag{12}$$

$$B_3 = \bar{B}_3 - \bar{Y} \tag{13}$$

The average response of each level of factor C is as follows:

$$\bar{C}_1 = {}^1/_9 \sum_{i=1}^{3} \sum_{j=1}^{3} Y_{1ij} \tag{14}$$

$$\bar{C}_2 = {}^1/_9 \sum_{i=1}^{3} \sum_{j=1}^{3} Y_{2ij} \tag{15}$$

$$\bar{C}_3 = {}^1/_9 \sum_{i=1}^{3} \sum_{j=1}^{3} Y_{3ij} \tag{16}$$

The main effect of each level of factor C is as follows:

$$C_1 = \bar{C}_1 - \bar{Y} \tag{17}$$

$$C_2 = \bar{C}_2 - \bar{Y} \tag{18}$$

$$C_3 = \bar{C}_3 - \bar{Y} \tag{19}$$

The average response of each combination of levels for factor A and B is as follows:

$$\overline{AB}_{ij} = {}^1/_3 \sum_{k=1}^{3} Y_{ijk} \tag{20}$$

The interaction effect for A and B is as follows:

$$AB_{ij} = \overline{AB}_{ij} - \bar{A}_i - \bar{B}_j + \bar{Y} \tag{21}$$

DOI: 10.21791/IJEMS.2026.09

The mean response of each set of levels for factor A and C is as follows:

$$\overline{AC}_{ik} = {}^{1}/_{3} \sum_{j=1}^{3} Y_{ijk} \tag{22}$$

The interaction effect for A and C is as follows:

$$AC_{ij} = \overline{AC}_{ik} - \overline{A}_i - \overline{C}_k + \overline{Y} \tag{23}$$

The mean response for each set of levels for factor B and C is as follows:

$$\overline{BC}_{jk} = {}^{1}/_{3} \sum_{i=1}^{3} Y_{ijk} \tag{24}$$

The interaction effect for B and C is as follows:

$$BC_{jk} = \overline{BC}_{jk} - \overline{B}_j - \overline{C}_k + \overline{Y} \tag{25}$$

The three-way interaction for A, B and C is as follows:

$$ABC_{jk} = Y_{ijk} - \overline{AB}_{ij} - \overline{AC}_{ik} - \overline{BC}_{jk} + \overline{A}_i + \overline{B}_j + \overline{C}_k - \overline{Y} \tag{26}$$

The coefficient of determination (R^2) is a statistical measure that provides insight into the goodness of fit of a regression model. An R^2 value of 1 indicates a perfect fit, meaning the model explains all the variability in the observed data. The expression for R^2 is given below.

$$R^2 = \frac{SS_{res}}{SS_{tot}} \tag{27}$$

Where

$$SS_{res} = \sum_{i=1}^{n} (y_i - \hat{y})^2 \tag{28}$$

$$SS_{tot} = \sum_{i=1}^{n} (y_i - \bar{y})^2 \tag{29}$$

$$\bar{y} = \frac{1}{n} \sum_{i=1}^{n} y_i \tag{30}$$

n = number of observations. The adjusted coefficient of determination (adjusted R^2) is defined as:

$$\bar{R}^2 = 1 - \frac{{}^{SS_{res}}/_{df_e}}{{}^{SS_{tot}}/_{df_i}} \tag{31}$$

where df_i - degrees of freedom for the model ($df_i = k$, where k is the number of predictors), df_e = degrees of freedom for error ($df_e = n - k - 1$, n = number of observations, k = number of explanatory variables).

DOI: 10.21791/IJEMS.2026.09

2. Results and Discussion

2.1. Influence of Surface Grinding Parameters on Apparent Elastic Modulus

The results for the effects of table speed, feed, and grinding depth on apparent elastic modulus (E) are shown in Table 5. The main effects plot for E is depicted in Figure 6. The main effects plot provides information on the degree of influence of the surface grinding parameters on the responses at low, moderate, and high levels.

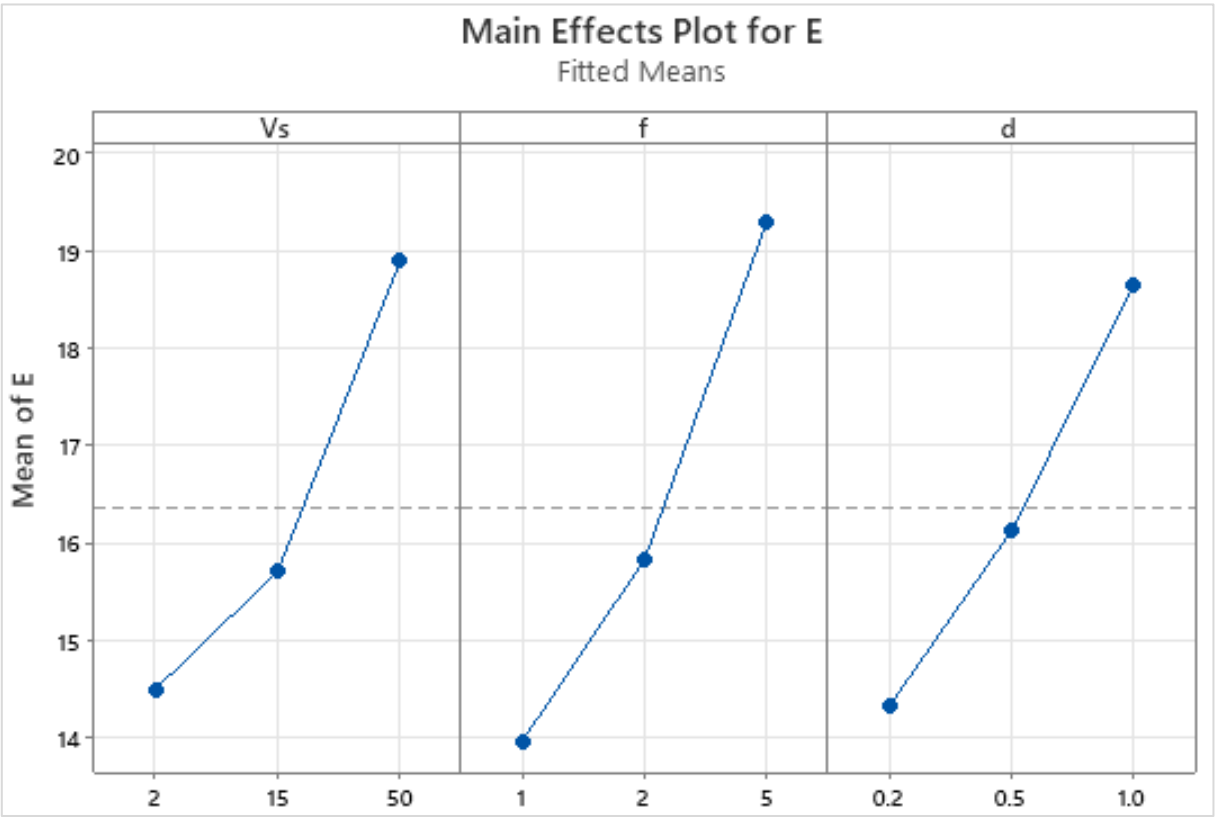

Figure 6. Main Effects Plot for Apparent Elastic Modulus

From Figure 6, the main effects plot for apparent elastic modulus (E) shows clear trends for table speed (V_s), feed rate (f), and grinding depth (d), with the overall mean apparent elastic modulus indicated at approximately 16.36 GPa. For table speed, the mean apparent elastic modulus increases from about 14.50 GPa at 2 spm to 15.71 GPa at 15 spm, and rises sharply to approximately 18.89 GPa at 50 spm, indicating a strong positive effect. This observation may be attributed to the fact that as the table speed increases, the grinding wheel does not have enough impact on the workpiece, and thus, the material hardness increases. Increasing material hardness also increases the apparent elastic modulus. A similar, more pronounced trend is observed for feed, where the mean apparent elastic modulus increases from roughly 13.97 GPa at 1.0 mm to 15.83 GPa at 2.0 mm, and reaches about 19.30 GPa at 5.0 mm, highlighting feed as the most influential parameter. The apparent elastic modulus of the material increases with grinding depth, from about 14.33 GPa at 0.2 mm to 16.12 GPa at 0.5 mm, and then to about 18.65 GPa at 1.0 mm, showing a positive but relatively weak dependence on grinding depth. The greater the grinding depth, the greater the strain hardening, so the apparent elastic modulus is greater. In general, the plot shows that the higher the value of all three grinding parameters, the higher the value

DOI: 10.21791/IJEMS.2026.09

of the apparent elastic modulus of AA7075 thin plates, and the maximum value is obtained when the grinding parameter of feed rate is higher. Overall, it can be seen that the greater the value of the three grinding parameters, the higher the value of the apparent elastic modulus of AA7075 thin plates, and the greater the value obtained by increasing the grinding parameter of feed rate, followed by table speed and grinding depth.

Runs	**Vs (spm)**	**f (mm)**	**d (mm)**	**E (GPa)**	
1	2	1	0.2	15.80	9.84
2	15	1	0.2	12.50	12.12
3	50	1	0.2	17.66	18.38
4	2	2	0.2	12.23	12.33
5	15	2	0.2	12.65	13.22
6	50	2	0.2	14.16	13.88
7	2	5	0.2	12.10	14.06
8	15	5	0.2	16.22	17.35
9	50	5	0.2	16.46	16.89
10	2	1	0.5	11.65	10.73
11	15	1	0.5	10.59	10.73
12	50	1	0.5	15.61	15.01
13	2	2	0.5	12.14	16.52
14	15	2	0.5	14.58	15.82
15	50	2	0.5	18.60	16.83
16	2	5	0.5	16.77	17.54
17	15	5	0.5	19.54	20.43
18	50	5	0.5	25.24	21.88
19	2	1	1	14.13	13.77
20	15	1	1	14.96	15.24
21	50	1	1	16.91	15.79
22	2	2	1	19.93	16.17
23	15	2	1	19.92	17.31
24	50	2	1	18.77	19.87
25	2	5	1	15.92	19.36
26	15	5	1	17.16	22.39
27	50	5	1	32.81	25.21

Table 5. Influence of Surface Grinding Parameters on Apparent Elastic Modulus of AA7075 Thin Plate

2.2. Identification of Significant Factors

2.2.1. Pareto Chart of Standardized Effects

In Figure 7, a Pareto chart of standardized effects (α = 0.05) is shown, plotting the relative importance of the main and interaction effects of the grinding parameters (interactions included for clarity) on the apparent elastic modulus (E). The vertical reference line is drawn at a standardized effect of 2.030, which is the threshold for a statistically significant effect. The most significant effects are the

DOI: 10.21791/IJEMS.2026.09

standardized effects, which are listed by the main effects, B with around 7.0 is the most influential main effect associated with the apparent elastic modulus. This is followed by **t**able speed (A) with a standardized effect of about 5.8, and grinding depth (C) with a value of 5.5, all of which exceed the significance threshold and are therefore statistically significant. In terms of interaction effects, the feed–grinding depth interaction (BC) shows a standardized effect of approximately 3.1, indicating a significant interaction influence on apparent elastic modulus.

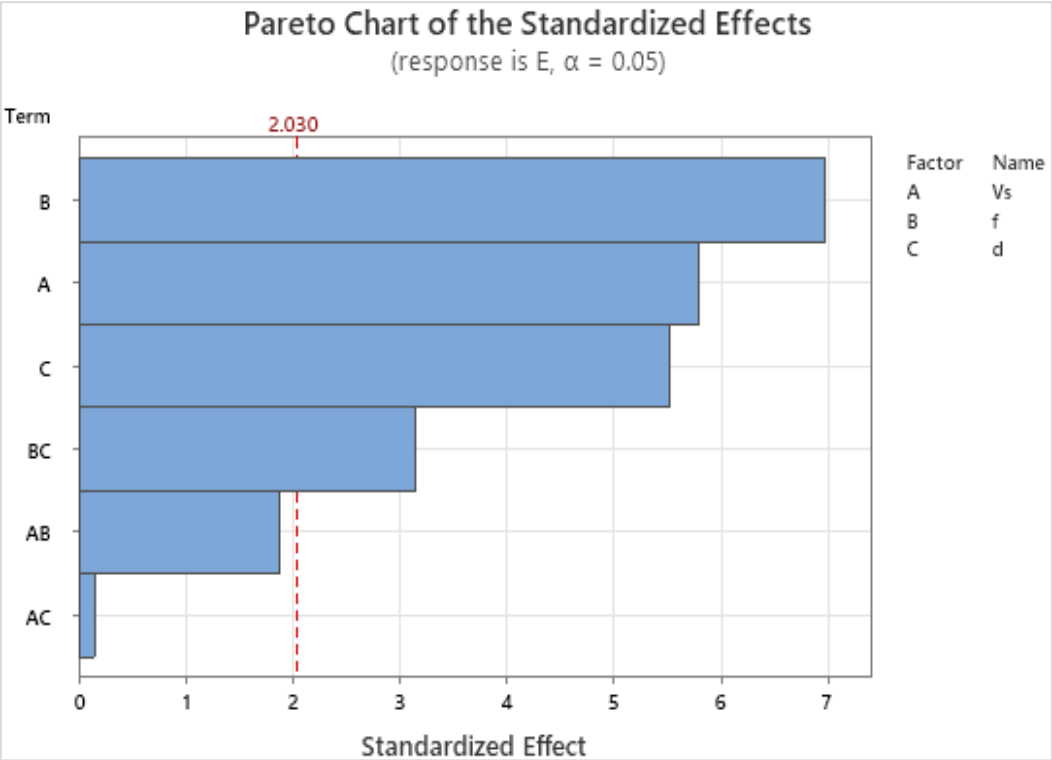

Figure 7. Pareto Chart of Standardized Effects on E

The table speed–feed interaction (AB), with a standardized effect of around 1.9, and the table speed–grinding depth interaction (AC), with a very small effect of 0.1, fall below the reference line and are thus considered statistically insignificant. Overall, the chart confirms that feed is the dominant factor influencing the apparent elastic modulus, followed by table speed and grinding depth, with only the feed–grinding depth interaction contributing significantly among the interaction terms.

2.2.2. Interaction Plot for Apparent Elastic Modulus

The interaction plot for apparent elastic modulus (E) in Figure 8, presents the combined effects of table speed (V_s), feed (f), and grinding depth (d) on the fitted mean response. The lines for the V_s–f and V_s–d interactions are basically parallel to each other over the range of levels studied, which confirms that the interactions are not significant on a statistical level and that their effects are minimal.

However, a clear deviation from parallelism is seen in the f–d interaction, the increase in apparent elastic modulus with grinding depth is more marked at higher feed, which suggests meaningful interaction between these two variables. In general, it could be concluded that apparent elastic modulus is affected mostly by the main effects of the grinding parameters and the feed–grinding depth interaction, while other interactions are negligible.

DOI: 10.21791/IJEMS.2026.09

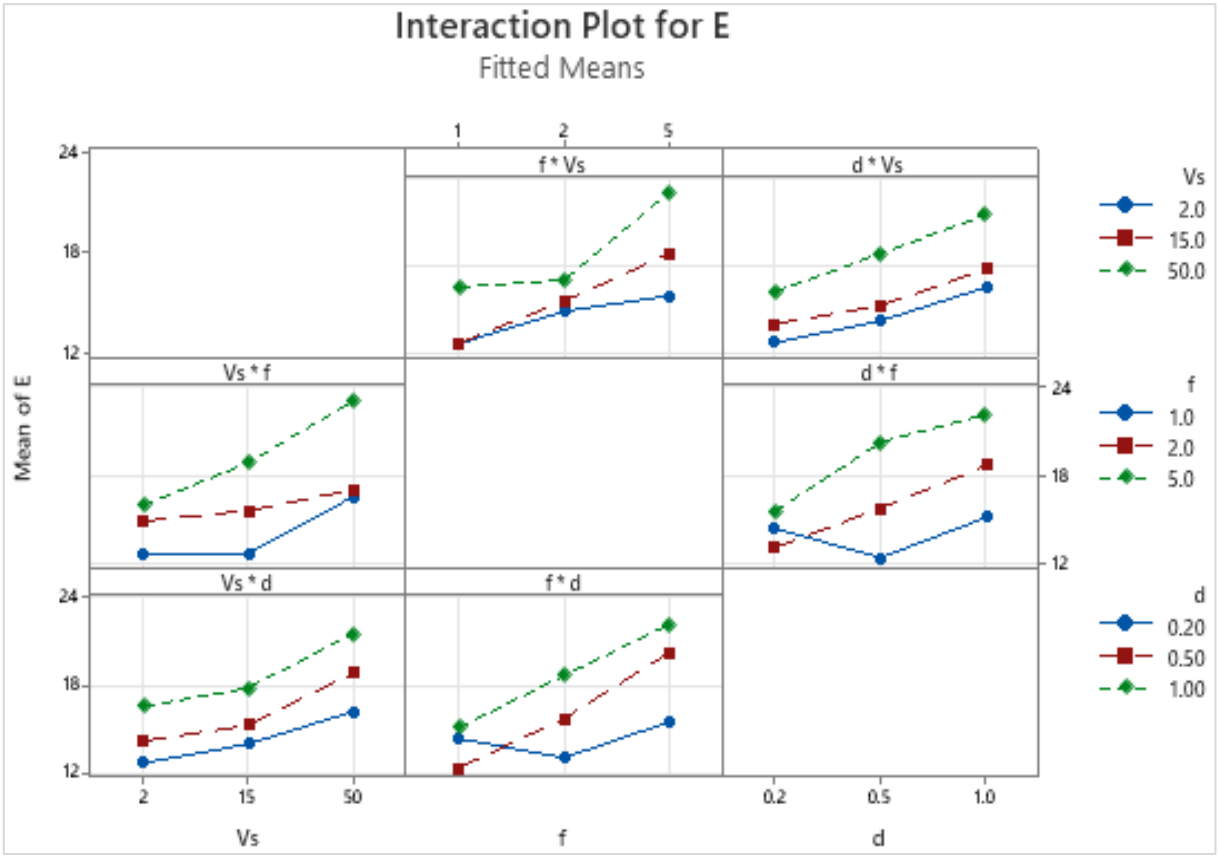

Figure 8. Interaction Plot for E

2.2.3. Coefficients of Apparent Elastic Modulus

The estimated regression coefficients of Table 6 indicate that the intercept term is statistically significant (16.364, at the 0.001 significance level), which corresponds to the response value at the reference values of table speed (Vs), feed (f), and grinding depth (d). For the main effects, Vs at 2 spm (−1.865, $p < 0.001$), f at level 1 mm (−2.397, $p < 0.001$), and d at 0.2 mm (−2.039, $p < 0.001$) exert statistically significant negative influences on the response, while Vs at 15 spm (−0.657, $p = 0.119$), f at level 2 mm (−0.535, $p = 0.202$), and d at 0.5 mm (−0.242, $p = 0.561$) are not significant. For the Vs–f interaction, the combinations Vs = 2 spm with f = 1 (0.551, $p = 0.350$) and f = 2 mm (0.922, $p = 0.122$), as well as Vs = 15 spm with f = 1 mm (−0.621, $p = 0.293$) and f = 2 mm (0.411, $p = 0.484$), are all statistically insignificant, indicating limited coupled influence between table speed and feed. Similarly, the Vs–d interactions at Vs = 2 spm with d = 0.2 mm (0.267, $p = 0.650$) and d = 0.5 mm (−0.033, $p = 0.955$), and at Vs = spm with d = 0.2 mm (0.342, $p = 0.560$) and d = 0.5 mm (−0.184, $p = 0.754$), show no significant effects. In contrast, the f–d interaction reveals a strong dependence on specific level combinations: f = 1 mm with d = 0.2 mm produces a significant positive effect (2.455, $p < 0.001$), whereas f = 1 mm with d = 0.5 mm yields a significant negative effect (−1.339, $p = 0.027$), while the combinations f = 2 mm with d = 0.2 mm (−0.712, $p = 0.229$) and f = 2 mm with d = 0.5 mm (0.161, $p = 0.784$) are not significant. The VIF values for all the terms are low (1.33–1.78), and this shows that there is no significant multicollinearity, further strengthening the robustness of the model estimates.

DOI: 10.21791/IJEMS.2026.09

Term	Coef	SE Coef	T-Value	P-Value	VIF
Constant	16.364	0.291	56.26	0.000	
Vs					
2	-1.865	0.411	-4.53	0.000	1.33
15	-0.657	0.411	-1.60	0.119	1.33
f					
1	-2.397	0.411	-5.83	0.000	1.33
2	-0.535	0.411	-1.30	0.202	1.33
d					
0.2	-2.039	0.411	-4.96	0.000	1.33
0.5	-0.242	0.411	-0.59	0.561	1.33
Vs*f					
2 1	0.551	0.582	0.95	0.350	1.78
2 2	0.922	0.582	1.59	0.122	1.78
15 1	-0.621	0.582	-1.07	0.293	1.78
15 2	0.411	0.582	0.71	0.484	1.78
Vs*d					
2 0.2	0.267	0.582	0.46	0.650	1.78
2 0.5	-0.033	0.582	-0.06	0.955	1.78
15 0.2	0.342	0.582	0.59	0.560	1.78
15 0.5	-0.184	0.582	-0.32	0.754	1.78
f*d					
1 0.2	2.455	0.582	4.22	0.000	1.78
1 0.5	-1.339	0.582	-2.30	0.027	1.78
2 0.2	-0.712	0.582	-1.22	0.229	1.78
2 0.5	0.161	0.582	0.28	0.784	1.78

Table 6. Coefficients of Apparent Elastic Modulus

2.2.4. Analysis of Variance (ANOVA) for Apparent Elastic Modulus

The ANOVA test shown in Table 7 indicates that the overall regression model is highly significant ($F = 9.18$, $p < 0.001$) and therefore very adequate at explaining the variation in the response. The linear effects are dominant, accounting for the greatest part of the explained variance (Adj SS = 617.722) and are highly statistically significant ($F = 22.53$, $p < 0.001$). Individually, table speed (Vs), feed (f), and grinding depth (d) all exert significant linear effects on the response, with feed showing the strongest influence (Vs: $F = 20.23$, $p < 0.001$; f: $F = 28.81$, $p < 0.001$; d: $F = 18.56$, $p < 0.001$). The two-way interaction terms are also significant ($F = 2.50$, $p = 0.017$), suggesting that the interactions of the factors are important beyond what is captured in the main effects. However, only the interaction between feed–grinding depth (f–d) is statistically significant ($F = 4.81$, $p = 0.003$), with the interaction between Vs–f being marginally significant ($F = 2.40$, $p = 0.069$) and the interaction between Vs–d being clearly insignificant ($F = 0.29$, $p = 0.884$). From the error analysis, it is seen that the lack of fit is not significant ($F = 2.02$, $p = 0.083$), indicating that the model explains the experimental data fairly well, and most of the variation is due to the pure error. Generally, these findings showed that the linear effect of Vs, f, and d are the main factors that govern the response, along with a significant interaction between feed and grinding depth.

DOI: 10.21791/IJEMS.2026.09

Source	DF	Adj SS	Adj MS	F-Value	P-Value
Model	18	754.659	41.926	9.18	0.000
Linear	6	617.722	102.954	22.53	0.000
Vs	2	184.892	92.446	20.23	0.000
f	2	263.248	131.624	28.81	0.000
d	2	169.582	84.791	18.56	0.000
2-Way Interactions	12	136.937	11.411	2.50	0.017
Vs*f	4	43.796	10.949	2.40	0.069
Vs*d	4	5.247	1.312	0.29	0.884
f*d	4	87.895	21.974	4.81	0.003
Error	35	159.930	4.569		
Lack-of-Fit	8	59.817	7.477	2.02	0.083
Pure Error	27	100.113	3.708		
Total	53	914.589			

Table 7. ANOVA for Apparent Elastic Modulus

2.3. Generation and Evaluation of Regression Model for E

The regression model obtained from Minitab 2021 software is shown as:

$$\begin{aligned} E = {} & 16.364 - 1.865\ Vs_2 - 0.657\ Vs_{15} + 2.522\ Vs_{50} - 2.397\ f_1 - 0.535\ f_2 + 2.932\ f_5 - 2.039\ d_{0.2} - \\ & 0.242\ d_{0.5} + 2.281\ d_{1.0} + 0.551\ Vs_2f_1 + 0.922\ Vs_2f_2 - 1.473\ Vs_2f_5 - 0.621\ Vs_{15}f_1 + 0.411\ Vs_{15}f_2 \\ & + 0.209\ Vs_{15}f_5 + 0.070\ Vs_{50}f_1 - 1.333\ Vs_{50}f_2 + 1.263\ Vs_{50}f_5 + 0.267\ Vs_2d_{0.2} - 0.033\ Vs_2d_{0.5} - \\ & 0.234\ Vs_2d_{1.0} + 0.342\ Vs_{15}d_{0.2} - 0.184\ Vs_{15}d_{0.5} - 0.158\ Vs_{15}d_{1.0} - 0.609\ Vs_{50}d_{0.2} + 0.217 \\ & Vs_{50}d_{0.5} + 0.392\ Vs_{50}d_{1.0} + 2.455\ f_1d_{0.2} - 1.339\ f_1d_{0.5} - 1.116\ f_1d_{1.0} - 0.712\ f_2d_{0.2} + 0.161 \\ & f_2d_{0.5} + 0.551\ f_2d_{1.0} - 1.743\ f_5d_{0.2} + 1.179\ f_5d_{0.5} + 0.564\ f_5d_{1.0} \end{aligned} \quad (32)$$

Where E = apparent elastic modulus; Vs = table speed; f = feed; and d = grinding depth

The model summary statistics indicate that the regression model captures the experimental data well. The standard error of the regression (S = 2.14) indicates that the average difference between the measured and predicted response values within the design space is relatively small, suggesting good prediction accuracy. The coefficient of determination (R^2 = 82.51%) indicates that the model accounts for a significant portion of the total variability in the response variable, confirming that the selected factors and interactions capture the main trends. When the number of model terms is taken into account, the adjusted coefficient of determination (R^2 adj = 73.52%) remains high, suggesting that the included predictors are important and that the model is not over-parameterized. The coefficient of determination (R^2 pred = 58.37%) is slightly lower than R^2 and R^2 adj, indicating a slight loss in predictive ability for new data, but it remains moderate. R^2(adj) is very similar to R^2(pred) for the experimental regression model, suggesting that the model is a good fit for the data from which it was created.

When looking at Table 8, the fits and diagnostics for the unusual observations (observations 26-28) suggest that there are a number of large residuals, as shown by the "R" flag. Note that the deviation between the experimental and fitted values, or residual, is large and negative (see Observation 26, residual = −4.38), and the standardized residual is negative (residual = −2.54), suggesting that at this condition the model is an over prediction of the response. In contrast, observation 27 exhibits a pronounced positive deviation (residual = 6.49) and a high standardized residual of 3.77, suggesting a

DOI: 10.21791/IJEMS.2026.09

significant under prediction by the model. Observation 28 also displays a notable negative residual (−3.50) with a standardized residual of −2.03. Standardized residuals exceeding ±2 typically signal potential outliers or influential observations, implying that these experimental runs are not well captured by the fitted model. While the presence of a small number of such observations does not invalidate the model, they warrant further examination to determine whether they arise from experimental variability, measurement error, or un-modeled process effects, and whether model refinement or additional terms could improve the fit.

Obs	E	Fit	Resid	Std Resid	
26	17.16	21.54	-4.38	-2.54	R
27	32.81	26.32	6.49	3.77	R
28	9.84	13.34	-3.50	-2.03	R

Table 8. Fits and Diagnostics for Unusual Observations

From Figure 9, the residual plots for E generally support the adequacy of the regression model, though a few limitations are noted. The normal probability plot shows that most standardized residuals lie close to the reference line, indicating that the normality assumption is reasonably satisfied, although slight deviations at the tails suggest the presence of a few extreme observations, consistent with the previously identified unusual runs.

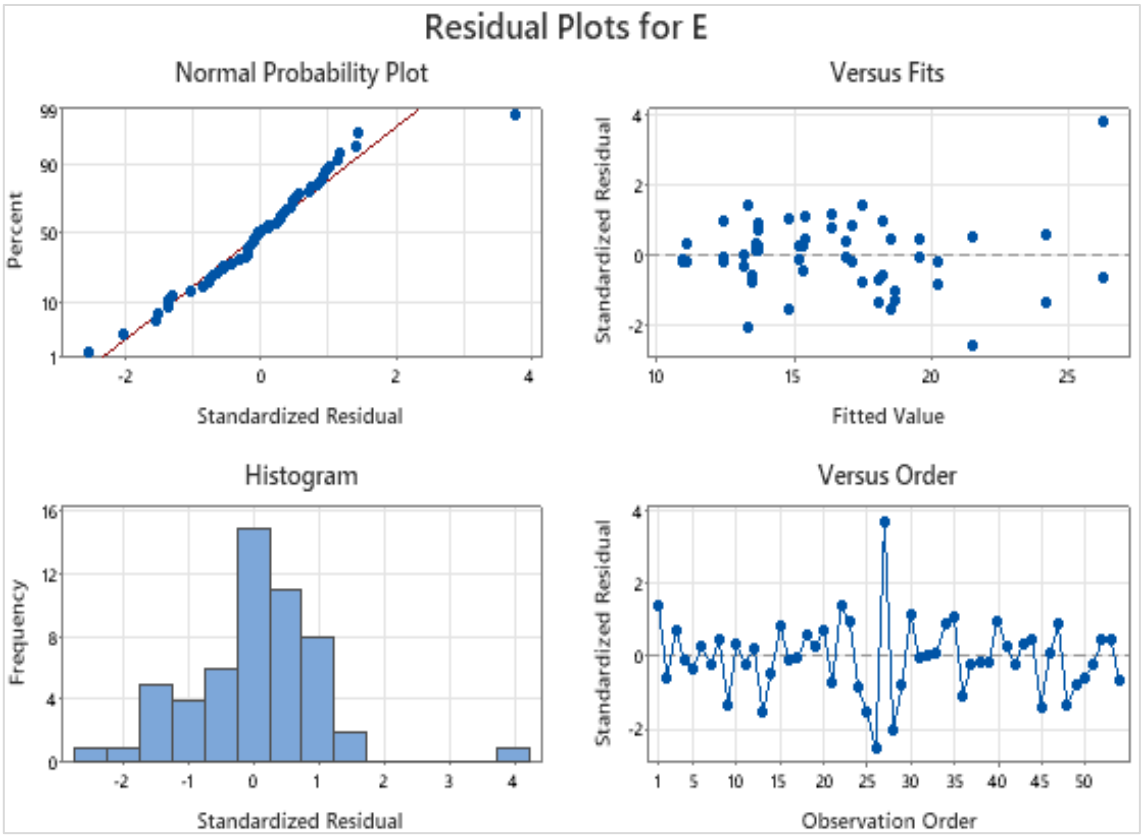

Figure 9. Residuals Plot for E

The histogram of standardized residuals is approximately symmetric and centered around zero, and thus, supports a near-normal error distribution. The plot of standardized residuals versus fitted values displays a random scatter about zero with no clear curvature or funnel shape, and this indicates that the assumptions of linearity and constant variance are largely met and that heteroscedasticity is not a major

DOI: 10.21791/IJEMS.2026.09

concern. Finally, the residuals versus order plot shows no systematic trend or cyclic pattern, indicating that the residuals are independent and that there are no time- or run-order-related effects influencing the response. Overall, the residual diagnostics indicate that the model assumptions are reasonably satisfied, although the presence of a few large residuals implies that certain experimental conditions are not perfectly captured and could be explored further for potential model refinement.

2.4. Optimization of Apparent Elastic Modulus

The optimization plot in Figure 10 shows that the apparent elastic modulus (E) is high with a desirability value of d ≈ 0.717 and a predicted maximum response of E ≈ 26.32. The optimal grinding conditions are found to be at high table speed (Vs) = 50 spm, high feed (f) = 5 mm, and high grinding depth (d) = 1 mm. This trend implies that as the grinding parameters increase, the stiffness also increases, and this could be due to surface and subsurface modifications that enhance strain hardening and microstructural refinement. The clustering of experimental points below the predicted optimum further confirms that the selected parameter combination yields the highest apparent elastic modulus among all tested conditions, making it particularly suitable for applications such as hydrofoil skin panels, where high stiffness and dimensional stability are critical.

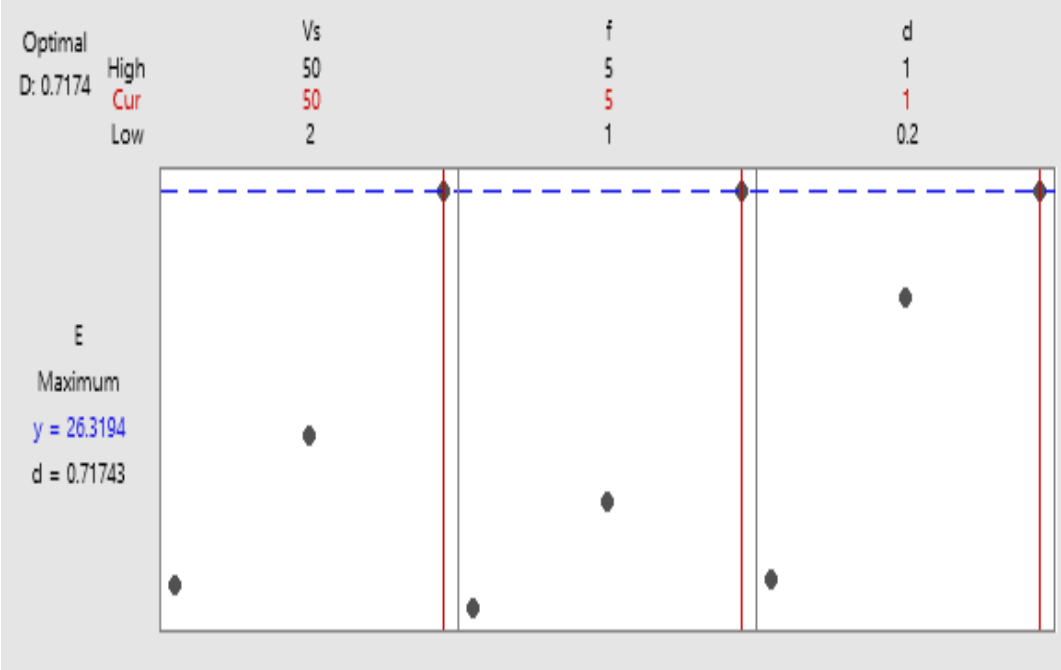

Figure 10. Optimization Plot for Apparent Elastic Modulus

Conclusions

Samples of AA7075 thin plates were ground according to a designed experimental plan, and their apparent elastic modulus was determined from the DI-CP/V2 Servo-hydraulic testing machine. The influence of table speed, feed and grinding depth on apparent elastic modulus was analyzed. The relevance of the main and interaction effects of the independent parameters on the apparent elastic modulus was analyzed. A regression model for apparent elastic modulus was generated and evaluated by Minitab 2021 software. The apparent elastic modulus was optimized to obtain favourable predictor

DOI: 10.21791/IJEMS.2026.09

settings for apparent elastic modulus. It was found that apparent elastic modulus is significantly influenced by all the three main grinding parameters, with feed exhibiting the highest standardized effect of approximately 7.0, followed by table speed at about 5.8 and grinding depth at roughly 5.5, all exceeding the statistical significance threshold of 2.030 at $\alpha = 0.05$, while only the feed–grinding depth interaction is significant among the interaction terms with a standardized effect of approximately 3.1, compared to the insignificant table speed–feed interaction (1.9) and table speed–grinding depth interaction (0.1). The developed regression model demonstrates a good fit to the experimental data, as reflected by a low standard error ($S = 2.14$), a high coefficient of determination ($R^2 = 82.51\%$), and a strong adjusted coefficient of determination (R^2 adj = 73.52%), indicating that the selected factors and interactions explain the majority of the variability in apparent elastic modulus. Although the predicted coefficient of determination is comparatively lower (R^2 pred = 58.37%), the difference between R^2 adj and R^2 pred remains within an acceptable range for experimental regression models, suggesting moderate predictive capability and indicating that removal of non-significant interaction terms could further improve model performance. The apparent elastic modulus (E) is high, with a desirability value of $d \approx 0.717$ and a predicted maximum response of $E \approx 26.32$. The optimal grinding conditions are found to be at high table speed (Vs) = 50 spm, high feed (f) = 5 mm, and high grinding depth (d) = 1 mm. These results show that increasing grinding severity enhances apparent elastic modulus, and this may be due to strain hardening and favourable surface and subsurface modifications. An optimized parameter window that produces high stiffness during surface grinding of AA7075 thin plates has been obtained to assist engineers in making concrete decisions. The study is limited to AA7075 thin plates and may not be applicable to other aluminum alloys or materials. Other factors, such as wheel dressing conditions, abrasion grain size, and vibration effects, which could have influenced the apparent elastic modulus, were not investigated. In the future, TEM (Transmission Electron Microscopy) or XRD (X-ray Diffraction) should be performed to correlate subsurface grain refinement (i.e. nanocrystals) or remaining compressive stress with the modification in the apparent elastic modulus. An improved elastic modulus measurement method incorporating machine compliance correction should be incorporated.

Author Contributions

Michael Boadu: Literature Review, Writing, Data interpretation, Methodology; Anthony Agyei-Agyemang: Project administration, Supervision; Faisal Adam: Co-supervision.

Funding

This research received no external funding.

Conflicts of Interest

The authors declare no conflicts of interest.

DOI: 10.21791/IJEMS.2026.09

References

[1] J. Joel and M. Anthony Xavior, "Aluminium Alloy Composites and its Machinability studies; A Review," *Materials Today: Proceedings*, vol. 5, no. 5, pp. 13556–13562, 2018, DOI: https://doi.org/10.1016/j.matpr.2018.02.351

[2] Z. B. Hou and R. Komanduri, "On the mechanics of the grinding process – Part I. Stochastic nature of the grinding process," *International Journal of Machine Tools and Manufacture*, vol. 43, no. 15, pp. 1579–1593, Dec. 2003, DOI: https://doi.org/10.1016/s0890-6955(03)00186-x

[3] K. Singh, A. Kumar, V. Sharma, and P. Kala, "Sustainable techniques in grinding: State of the art review," *Journal of Cleaner Production*, vol. 269, p. 121876, Oct. 2020, DOI: https://doi.org/10.1016/j.jclepro.2020.121876

[4] Instron, "Modulus of Elasticity," *Instron*, Apr. 18, 2024. https://www.instron.com/en/resources/glossary/modulus-of-elasticity/

[5] S. Hill, "A Guide to Young's Modulus and Material Stiffness," *BES Group*, Mar. 26, 2025. https://besgroup.com/blogs/a-guide-to-youngs-modulus-and-material-stiffness/

[6] M. Boadu, A. Agyei-Agyemang, P. Andoh, and F. Adam, "Assessment of Mechanical Behaviour Trends of Surface-Ground AA7075 Thin Plate Across Run Orders," *Advances in Mechanical and Materials Engineering*, vol. 43, pp. 29–42, Jan. 2026, DOI: https://doi.org/10.7862/rm.2026.3

[7] D. Hou, S. Gao, J. Liu, and S. Huang, "Effect of Grinding Parameters on the Hardness Penetration Depth of the Steel GCr15 in Internal Grind Hardening Process," *Journal of Physics Conference Series*, vol. 1637, no. 1, pp. 012112–012112, Sep. 2020, doi: https://doi.org/10.1088/1742-6596/1637/1/012112

[8] S. Guo, S. Lu, B. Zhang, and C. F. Cheung, "Surface integrity and material removal mechanisms in high-speed grinding of Al/SiCp metal matrix composites," *International Journal of Machine Tools and Manufacture*, vol. 178, p. 103906, Jul. 2022, doi: https://doi.org/10.1016/j.ijmachtools.2022.103906

[9] M. Beghini, L. Bertini, B. D. Monelli, C. Santus, and M. Bandini, "Experimental parameter sensitivity analysis of residual stresses induced by deep rolling on 7075-T6 aluminium alloy," *Surface and Coatings Technology*, vol. 254, pp. 175–186, Sep. 2014, doi: https://doi.org/10.1016/j.surfcoat.2014.06.008

[10] El Ouafi and N. Barka, "Un modèle intégré pour la prédiction de l'état de surface en fraisage pour alliages d'aluminium," *Revue de Métallurgie*, vol. 108, no. 6, pp. 357–368, 2011, DOI: https://doi.org/10.1051/metal/2011070

[11] E. M. Anderson, J. R. Niska, and E. E. Niska, "Factorial design," Academic Press, 2023, pp. 327– 330. DOI: https://doi.org/10.1016/B978-0-323-88423-5.00110-2

[12] B209, ''Standard Specification for Aluminum and Aluminum-Alloy Sheet and Plate'', *American Society for Testing and Materials*, 100 Barr Harbor Dr., West Conshohocken, PA 19428, 2014.

DOI: 10.21791/IJEMS.2026.09

[13] N. M. Vaxevanidis, N. A. Fountas, C. Koraidis, A. Koutsomichalis, & P. Psyllaki, ‘‘Modeling of surface finish in turning of a brass alloy based upon statistical multi-parameter analysis’’, *Tribological Journal BULTRIB*, vol. 5, pp. 303-313, 2015.

[14] BS 1SO 6892-1:2019, “Metallic Materials – Tensile Testing. Part 1: Method of Test at Room Temperature’’, *British Standards Institution (BSI) Limited*, 2020.

[15] L. M. Robert, F. G. Richard, and L. H. James, Statistical and Analysis of Experiments. New York: John Wiley and Sons Publication, 2003.